JOURNAL OF GEOPHYSICAL RESEARCH, VOL. 106, NO. D15, PAGES 17,403–17,419, AUGUST 16, 2001

Generalized model for NO_x and N_2O emissions from soils

W. J. Parton,[1] E. A. Holland,[1,2,3] S. J. Del Grosso,[1] M. D. Hartman,[1] R. E. Martin,[4] A. R. Mosier,[5] D. S. Ojima,[1] and D. S. Schimel,[1,2,3]

Abstract. We describe a submodel to simulate NO_x and N_2O emissions from soils and present comparisons of simulated NO_x and N_2O fluxes from the DAYCENT ecosystem model with observations from different soils. The N gas flux submodel assumes that nitrification and denitrification both contribute to N_2O and NO_x emissions but that NO_x emissions are due mainly to nitrification. N_2O emissions from nitrification are calculated as a function of modeled soil NH_4^+ concentration, water-filled pore space (WFPS), temperature, pH, and texture. N_2O emissions from denitrification are a function of soil NO_3^- concentration, WFPS, heterotrophic respiration, and texture. NO_x emissions are calculated by multiplying total N_2O emissions by a NO_x:N_2O equation which is calculated as a function of soil parameters (bulk density, field capacity, and WFPS) that influence gas diffusivity. The NO_x submodel also simulates NO_x emission pulses initiated by rain events onto dry soils. The DAYCENT model was tested by comparing observed and simulated parameters in grassland soils across a range of soil textures and fertility levels. Simulated values of soil temperature, WFPS (during the non-winter months), and NO_x gas flux agreed reasonably well with measured values (r^2 = 0.79, 0.64, and 0.43, respectively). Winter season WFPS was poorly simulated (r^2 = 0.27). Although the correlation between simulated and observed N_2O flux was poor on a daily basis (r^2=0.02), DAYCENT was able to reproduce soil textural and treatment differences and the observed seasonal patterns of gas flux emissions with r^2 values of 0.26 and 0.27, for monthly and NO_x flux rates, respectively.

1. Introduction

Our understanding of the terrestrial nitrogen (N) cycle has increased dramatically over the past two decades [*Holland et al.*, 1999; *Vitousek et al.*, 1997; *Howarth et al.*, 1996]. This has laid the groundwork for investigating a wide spectrum of environmental issues including water, soil, and air pollution and has allowed the development of comprehensive budgets of N gas fluxes. A number of models link nitrous oxide (N_2O) production in soil to the physically regulated biotic N cycle [*Frolking et al.*, 1998]. These and other models range from the highly mechanistic that explicitly represent the biological and physical processes that control N dynamics [*Grant and Pattey*, 1999] to simpler models that simulate N cycling as a function of organic matter decomposition rates and environmental variables such as soil water and temperature [*Li et al.*, 1992; *Parton et al.*, 1996].

Nitric oxide (NO) plays a major role in lower atmospheric chemistry [*Brasseur et al.*, 1999]. The formation of ozone (O_3) and the overall oxidizing capacity of the troposphere are limited by the availability of NO and its oxidized counterpart, NO_2, which together are referred to as NO_x [*Williams et al.*, 1992]. The effects of increased NO_x emissions range from tropospheric O_3 pollution, a continuing problem in urban areas throughout the world, to acid deposition, which can influence the structure and function of ecosystems in remote areas [*Holland and Lamarque*, 1997; *Levy et al.*, 1997; *Chameides et al.*, 1994]. Prehistoric atmospheres likely relied on natural sources of NO_x such as lightning, biomass burning, and biological production to maintain atmospheric O_3 and OH^- concentrations [*Madronich and Hess*, 1994; *Hauglustaine et al.*, 1999]. Anthropogenic sources (mainly fossil fuel burning) are thought to be responsible for 50% or more of modern day inputs of NO_x to the troposphere [*Prather et al.*, 1995], while emissions from soils contribute 10 to 40% of the total [*Davidson and Kingerlee*, 1997]. N_2O has a much longer residence time in the atmosphere than NO_x (120 years versus less than 1 week [*Prather et al.*, 1995]), and it is an important greenhouse gas. N_2O also regulates stratospheric O_3 concentrations. Soil emissions of N_2O are thought to be a major source of both anthropogenic and natural N_2O production [*Kroeze et al.*, 1999]. Models of NO_x and N_2O emissions are needed to better assess the contributions of human activity on N budgets and better quantify the feedbacks between increased nitrogen gas concentrations in the atmosphere and accelerated cycling of N through the biosphere.

Estimates of NO_x emissions from soils range from 3.3 Tg NO_x-N yr^{-1} [*Yienger and Levy*, 1995] to 21 Tg NO_x -N yr^{-1} [*Davidson and Kingerlee*, 1997] of total global NO_x inputs to the atmosphere of ~50 Tg NO_x-N yr^{-1} [*Prather et al.*, 1995]. Estimates of total atmospheric N_2O inputs range from 10 to 17 Tg N_2O-N yr^{-1} and over half of these inputs are thought to

[1]Natural Resource Ecology Laboratory, Colorado State University, Fort Collins, Colorado.
[2]Max Planck Institut fur Biogeochemie, Jena, Germany.
[3]National Center for Atmospheric Research, Boulder, Colorado
[4]Cooperative Institute for Research in Environmental Sciences, University of Colorado, Boulder, Colorado.
[5]Agriculture Research Service, U.S Department of Agriculture, Fort Collins, Colorado.

Paper number 2001JD900101.
0148-0227/01/2001JD900101$09 00

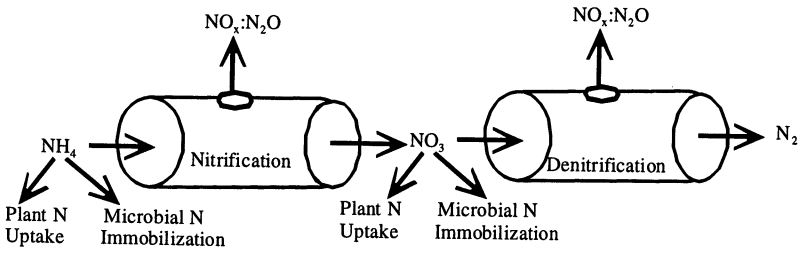

Figure 1. Conceptual model of controls on N gas emissions from soil using the leaky pipe metaphor of *Firestone and Davidson* [1989]. The total N gas emitted from the soil is proportional to the amount of N cycling through the pipe, while the proportions of NO, N_2O, and N_2 emitted from the soil are controlled by soil water content and soil physical properties that influence gas diffusivity. Figure 1 is a modification of a figure from *Davidson* [1991].

originate from soils [*Prather et al.*, 1995]. There have been a number of exercises aimed at developing regional and global inventories of NO_x and N_2O emissions from soils [*Delmas et al.*, 1997; *Lee et al.*, 1997; *Mosier et al.*, 1998]. Attempts to quantify soil global NO_x and N_2O emissions have ranged from compilations of small-scale measurements [*Davidson*, 1993; *Davidson and Kingerlee*, 1997] to more process-based estimates [*Li et al.*, 2000; *Potter et al.*, 1996a]. In some cases the inventories [*Yienger and Levy*, 1995] have been used as inputs for chemical transport models which are an important tool for elucidating the impact of human activities on the Earth's chemical environment [*Prather et al.*, 1999; *Hauglustaine et al.*, 1998].

NO_x and N_2O are produced in soils as obligate intermediates or by-products of the microbially mediated processes of nitrification and denitrification [*Conrad*, 1996]. Figure 1 shows the flows of N in soil and the major controls on nitrification and denitrification. Nitrification is an aerobic process that is primarily carried out by autotrophic bacteria resulting in the conversion of NH_4^+ to NO_3^- through the intermediate NO_2^-. In addition, heterotrophic nitrification by fungi may be important in acidic forest soils [*Schimel et al.*, 1984]. Denitrification is an anaerobic process in which nitrogen oxides (NO_3^-, NO_2^-, NO_x, N_2O) are used as terminal electron acceptors during fermentation of organic substrates. The complete denitrification pathway results in the reduction of NO_3^- to N_2, but significant amounts of N_2O, as well as small amounts of NO_x, may be emitted before complete reduction to N_2. Factors that control nitrification and denitrification rates in soil include concentration of the respective forms of mineral N (NH_4^+ and NO_3^-), soil water content, temperature, labile carbon availability (for denitrification), and soil physical properties related to texture that influence gas diffusion rates [*Robertson and Tiedje*, 1987]. Conceptually, our N gas model is based on the leaky pipe metaphor of *Firestone and Davidson* [1989] in which total N gas emissions from soil are proportional to N cycling and soil gas diffusivity determines the relative amounts of the respective N gas species emitted (Figure 1).

Here we describe an updated version of the nitrification/denitrification submodel for N_2O emissions developed by *Parton et al.* [1996] and describe a new submodel for simulating NO_x emissions associated with nitrification. The new submodel assumes that N_2O emissions are proportional to nitrification and denitrification rates and that the ratio of NO_x to N_2O emitted from soil is controlled by gas diffusivity. The updated submodel has been incorporated into the new daily version of the CENTURY model (DAYCENT). DAYCENT has been used to simulate plant production and trace gas fluxes from a variety of natural and managed ecosystems [*Kelly et al.*, 2000; *Frolking et al.*, 1998]. In this paper we compare observations and simulations of soil temperature, H_2O, soil mineral N levels, NO_x and N_2O fluxes for five different grassland sites across a range of soil textures from sandy loam to clay loam and including fertilized and unfertilized pastures [*Martin et al.*, 1998; *Mosier et al.*, 1996].

2. Materials and Methods

2.1 DAYCENT Model

DAYCENT [Del Grosso et al., 2001; *Kelly et al.*, 2000; *Parton et al.*, 1998] is an ecosystem model used to simulate terrestrial C, N, P, and S dynamics and includes submodels for soil organic matter (SOM) decomposition, land surface parameters, plant productivity, and trace gas fluxes (Figure 2). The land surface submodel of DAYCENT simulates water content and temperature for various soil layers and evapotranspiration using daily precipitation and maximum/minimum air temperature data as drivers. The plant production submodel uses soil water content, temperature, and available nutrients to calculate plant growth, and C is allocated among leafy, woody, and root biomass based on vegetation type. Soil water content and temperature control the death rate of plant components. Dead plant material is divided into structural (high C:N) and metabolic (low C:N) components. Decomposition of dead plant material supplies the SOM pool. Soil organic matter is divided into three pools (active, slow, and passive) based on turnover rates. N mineralization, N fixation, N fertilization, and N deposition supply the available nutrient pool. NO_3^- is distributed throughout the soil profile while NH_4^+ is modeled only for the top 15 cm layer. NO_3^- and NH_4^+ are available for plant uptake and for biochemical processes (nitrification and denitrification) that result in N gas emissions. Soil physical properties, environmental variables, and lignin and N concentrations of vegetation, litter and SOM drive the flows of nutrients through the pools.

The N gas submodel of DAYCENT uses calculated soil water content, temperature, NH_4^+, NO_3^-, and respiration to drive simulations of daily N_2O and NO_x emissions from nitrification and denitrification. A daily time step is used because this degree of resolution is needed to simulate the short-term events that are often responsible for the majority of N gas emissions from soils [*Martin et al.*, 1998; *Frolking et al.*, 1998]. First, total N_2O emissions from nitrification and

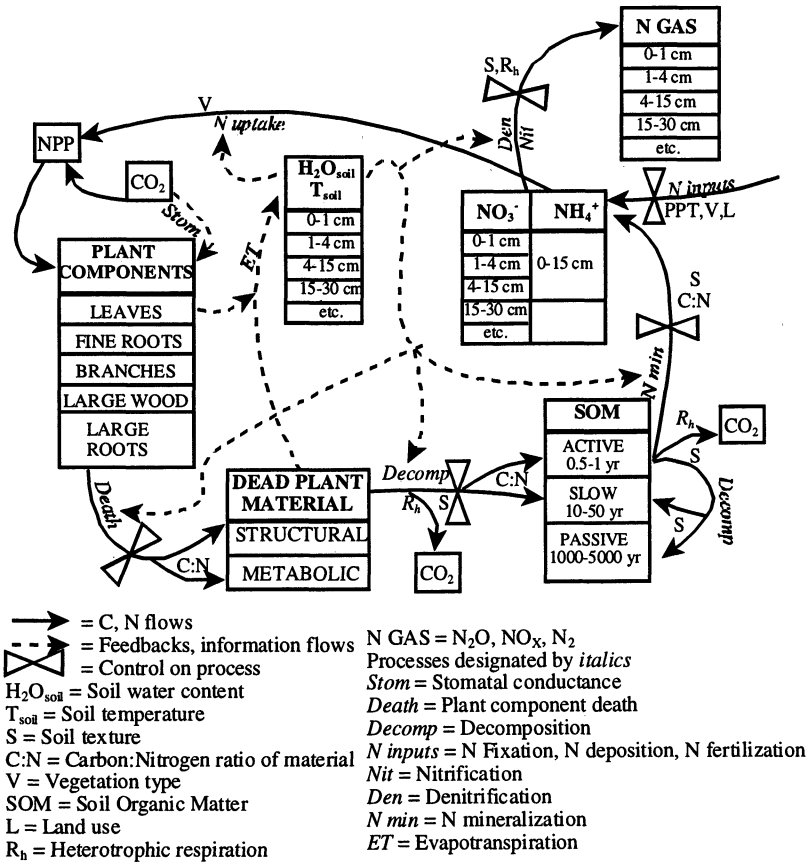

Figure 2. Flow diagram for the DAYCENT ecosystem model.

denitrification are calculated, then the NO_x to N_2O ratio function is used to calculate NO_x emissions.

The latest version of DAYCENT used for the simulations reported in this paper included changes in the snowmelt infiltration submodel and submodels used to calculate N gas emissions. Comparisons of simulated and observed soil water-filled pore space (WFPS) values from data not reported in this paper showed that the model was biased in that winter season WFPS values were underestimated. Data analysis showed that low WFPS estimates in winter resulted from most of the snowmelt running off of the soil surface. To correct this problem, the algorithm controlling snowmelt infiltration was changed and the minimum hydraulic conductivity of frozen soils was increased. The time allowed for water infiltration to occur was increased for the days the ground is covered by a snowpack. The impedance to water infiltration is now calculated on a smaller timescale, and the snowmelt algorithm is now based on maximum daily soil temperature rather than mean daily soil temperature.

2.2. Denitrification Submodel

The submodel for N_2O and N_2 flux from denitrification [*Del Grosso et al.*, 2000; *Parton et al.*, 1996] assumes that N gas flux from denitrification is controlled by soil NO_3^- concentration (e^- acceptor), labile C availability (e^- donor), and O_2 availability (competing e^- acceptor). Soil NO_3^- concentration is simulated by DAYCENT and simulated heterotrophic CO_2 respiration is used as a surrogate for labile C availability. The O_2 status of the soil is calculated as a function of WFPS, soil physical properties that control gas diffusivity, and O_2 demand. Gas diffusivity, normalized to soil water content at field capacity, is controlled by soil bulk density and field capacity. O_2 demand is a function of simulated heterotrophic respiration rates.

The denitrification submodel assumes that the process is controlled by the molecular species (NO_3^-, labile C) or environmental condition (O_2 availability) that is most limiting. The denitrification equation selects the minimum of the NO_3^- and CO_2 functions to calculate a maximum denitrification rate for particular levels of e^- acceptor and e^- donor. The calculated maximum denitrification rate is then attenuated by a multiplier that reflects O_2 availability. When WFPS is less than ~55%, no denitrification is assumed to occur. In the interval ~55% < WFPS < ~90% denitrification rates increase exponentially and the rate of increase levels off as soils approach saturation. The denitrification WFPS curve reported in Figure 7 of *Del Grosso et al.* [2000] was slightly altered so that denitrification does not occur, as opposed to simulating minimal rates, at WFPS < ~55%. The modified denitrification water function is

$$y = 0.5 \operatorname{atan}(0.6\pi\ (0.1x - a))/\pi, \quad (1)$$

where y is the relative denitrification rate, x is the simulated WFPS, and a controls the WFPS level at which denitrification is assumed to reach half of its maximum rate. The parameter a is calculated as a function of soil gas diffusivity and heterotrophic respiration. In soils with low gas diffusivity, a is assumed to occur at lower WFPS levels when O_2 demand is

high because atmospheric O_2 may not diffuse into the soil fast enough to fully satisfy microbial demand. Consequently, some microsites may become anoxic and support denitrification at relatively low WFPS levels.

After calculating $N_2 + N_2O$ emissions from denitrification, an N_2 to N_2O ratio function is used to infer the proportion of denitrification N gas losses that are in the form of N_2 and N_2O. The submodel assumes that as O_2 availability decreases and as the ratio of e^- donor to e^- acceptor increases a larger proportion of N_2O from denitrification will be further reduced to N_2 before diffusing from the soil to the atmosphere. This is based on the relative affinities for enzymes to use O_2, NO_3^-, and N_2O as e^- acceptors when labile C is available.

2.3. Nitrification Submodel

Parton et al. [1996] and other authors have shown that soil nitrification rates are controlled by the soil NH_4^+ concentration [*Smart et al.*, 1999], water content [*Davidson*, 1993], temperature [*Martin et al.*, 1998; *Skiba et al.*, 1992], and pH [*Ellis et al.*, 1997; *De Groot et al.*, 1994]. We use a revised version of equations developed by *Parton et al.* [1996] to simulate soil nitrification rate as a function of these factors using (2).

$$FNO_3 = Net_{min} * K_1 + K_{max} * NH_4 * F(t) * F(WFPS) * F(pH), \quad (2)$$

where FNO_3 is the soil nitrification rate (gN m^{-2} d^{-1}), Net_{min} is the daily net N mineralization from the SOM decomposition submodel, K_1 is the fraction of Net_{min} that is assumed to be nitrified each day (K_1 = 0.20), NH_4 is the model-derived soil ammonium concentration (gN m^{-2}), K_{max} is the maximum fraction of NH_4^+ nitrified (K_{max} = 0.10 d^{-1}), $F(t)$ is the effect of soil temperature on nitrification (Figure 3a), F(WFPS) is the effect of soil water content and soil texture on nitrification (Figure 3b), and F(pH) is the effect of soil pH on nitrification (Figure 3c). The effect of soil temperature on nitrification is based on data presented by *Malhi and McGill* [1982] which show that there is an optimal temperature for nitrification that is a function of the average maximum monthly air temperature for the warmest month of the year. This function is based on data from three sites but appears to be consistent with data from other sites [*Stark*, 1996; *Singh et al.*, 1993]. The effect of WFPS on nitrification is based on data presented by *Doran et al.* [1988] and changes as a function of soil texture. F(pH) uses the same equation presented by *Parton et al.* [1996], while K_{max} was estimated by using data from *Malhi and McGill* [1982]. K_1 was calibrated from comparisons of simulated N_2O emissions and N_2O flux data from grassland soils during 1990-1993 [*Mosier et al.*, 1996]. We assume that N_2O flux from nitrification is proportional to the nitrification rate and calculate flux using (3).

$$FN_2O = K_2 * FNO_3 \quad (3)$$

FN_2O is the N_2O flux from nitrification (gN m^{-2} d^{-1}), K_2 is the fraction of nitrified N lost as N_2O flux (K_2 = 0.02) and FNO_3 is the nitrification rate as calculated by (1). The value for K_2 was estimated by comparing observed N_2O flux data [*Mosier et al.*, 1996] with simulated model results [*Frolking et al.*, 1998].

2.4. NO_x:N_2O Data Analysis

Potter et al. [1996a] proposed a model where the NO_x to N_2O ratio is a function of WFPS. The *Potter et al.* [1996a] model assumes that NO_x:N_2O is maximum at low WFPS and decreases as WFPS increases with NO_x and N_2O emissions being equal at approximately 60% WFPS. The decrease NO_x:N_2O with increasing WFPS is thought to be a result of decreasing soil gas diffusivity [*Potter et al.*, 1997; *Schuster and Conrad*, 1992]. This is supported by observations that nitrification is the primary contributor to N gas flux when soils have abundant oxygen while denitrification is the primary contributor under anaerobic conditions [*Linn and Doran*, 1984; *Davidson*, 1993] and that measured NO_x emissions from soils are due primarily to nitrification because NO_x is highly reactive under the reducing conditions that facilitate denitrification [*Conrad*, 1996]. As soil gas diffusivity decreases a larger proportion of the soil volume is expected to become depleted in O_2 which facilitates denitrification and inhibits nitrification, thus implying that more N_2O is released from soil relative to NO_x.

The new NO_x flux model was developed using observed NO_x:N_2O gas flux data as a function of soil properties from various ecosystems. The sites included a sandy soil from South Africa [*Scholes et al.*, 1997], sandy loam (fertilized and native), sandy clay loam (fertilized and native) and clay loam sites from Colorado [*Martin et al.*, 1998; *Mosier et al.*, 1996, 1997, 1998], a spruce forest in Germany [*Papen and Butterbach-Bahl*, 1999; *Gasche and Papen*, 1999], volcanic soils in Costa Rica [*Veldkamp et al.*, 1998; *Veldkamp and Keller*, 1997; *Keller et al.*, 1993], and tropical agricultural soils in Mexico [*Matson et al.*, 1998]. We only used data for observations where both NO_x and N_2O were measured at the same time and excluded data collected when temperatures were below freezing (negative NO_x fluxes frequently occur during winter). Data points with N_2O fluxes less than 0.2 gN ha^{-1} d^{-1} for the Colorado soils and less than 0.4 gN ha^{-1} d^{-1} for the other soils were eliminated because flux values in these ranges are close to the detection limits of the measurement methods used. We also eliminated data points with NO_x:N_2O greater than two standard deviations above the mean for each soil texture/water content class to reduce some of the variability associated with trace gas flux measurements. For each observation considered, soil gas diffusivity (D/D_o) and WFPS were calculated. WFPS was calculated as a function of measured soil bulk density (BD) and gravimetric soil water content (Θ_g) using (4):

$$WFPS = \Theta_g * BD/(1-BD/2.65). \quad (4)$$

D/D_o, a relative index of gas diffusivity in soil, was calculated using equations presented by *Potter et al.* [1996b] which are based on an algorithm described by *Millington and Shearer* [1971]. D/D_o is assumed to be a function of WFPS, BD, and water content at field capacity (FC). Values for BD and FC were derived from field measurements of BD and water content and from standard values based on soil texture classification [*Saxton et al.*, 1986]. D/D_o accounts for air-filled pore space and pore size distribution. D/D_o decreases as WFPS or BD increases because air-filled pore space decreases. D/D_o decreases as FC increases because higher FC is associated with a larger proportion of micropores which do not facilitate gas diffusivity as well as macropores. D/D_o should represent the O_2 status of the soil better than WFPS because it accounts for pore size distribution, total pore space, and air-filled pore space, whereas WFPS accounts only for the latter two factors.

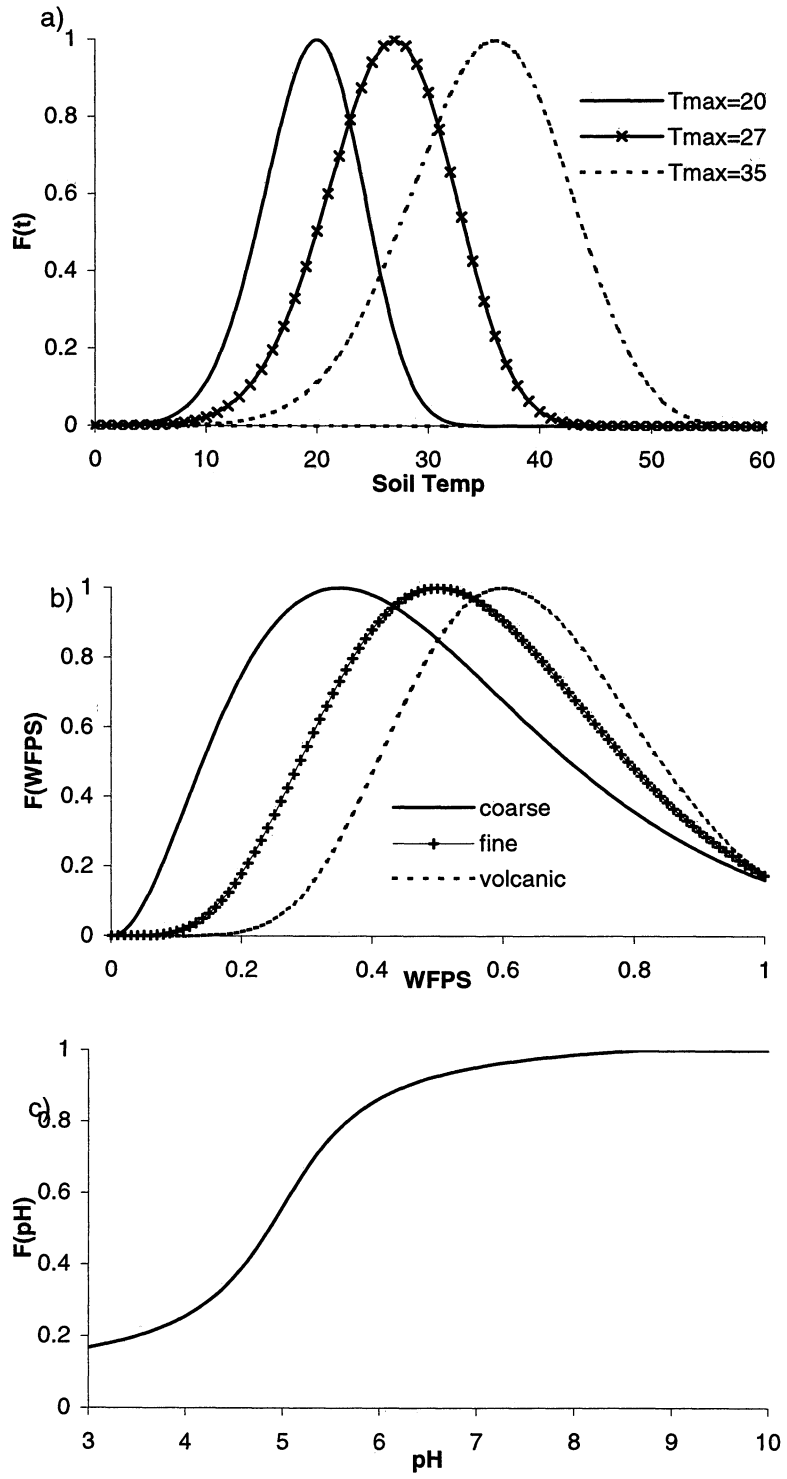

Figure 3. Effect of (a) soil water-filled pore space, (b) soil temperature, and (c) soil pH on nitrification.

There are general patterns of decreasing NO_x to N_2O ratios with increasing WFPS and decreasing D/D_o values but NO_x:N_2O for the aggregated data from all of the soils is quite variable (Figures 4a and 4b). D/D_o is better correlated to the ratio than WFPS (r^2 = 0.40 versus 0.28), but there is substantial unexplained variability in both cases (Figure 4). Overall, NO_x:N_2O decreases with increasing water content. When plotted for each soil texture class, the ratio is highest for coarse-textured soils and lowest for fine-textured soils.

To consider both WFPS and the constraints on soil gas diffusivity represented by D/D_o, we grouped the data for each site into classes based on WFPS, and then derived the relationship between NO_x:N_2O and D/D_o. D/D_o is clearly related to water-filled pore space (Figure 4c). For each soil, data were divided into groups based on WFPS (10% increments for most sites) and NO_x to N_2O ratios for all of the observations within the WFPS groups were averaged. Average NO_x to N_2O ratios were plotted versus D/D_o averages

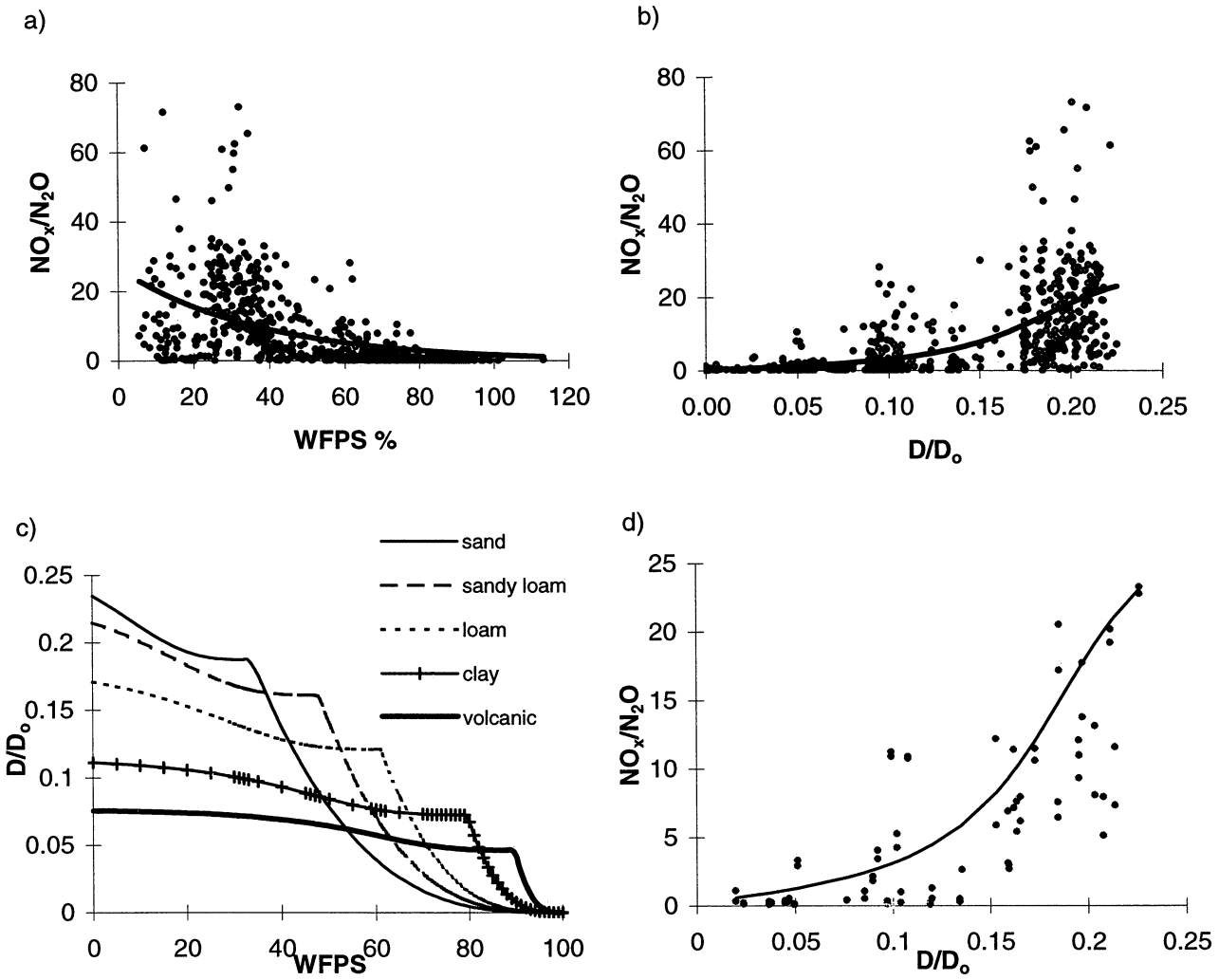

Figure 4. (a) Effect of soil WFPS on the NO_x/N_2O ratio and best fitting exponential function ($r^2 = 0.28$). (b) Effect of soil gas diffusivity D/D_o on the NO_x/N_2O ratio and best fitting arctangent function ($r^2 = 0.40$). (c) Values of D/D_o calculated for various soils as a function of WFPS, bulk density, and field capacity using an equation presented by *Potter et al.* [1996a]. (d) Effect of D/D_o on average NO_x/N_2O ratios based on WFPS classes and the arctangent function from Figure 4b ($r^2 = 0.63$).

for the soil groups based on WFPS (Figure 4d). Using group average values for NO_x:N_2O greatly decreased variability and improved the correlation with D/D_o. NO_x:N_2O was minimal (< 0.5) at D/D_o values below 0.1 and increased gradually in the interval of $0.1 < D/D_o < 0.2$. The arctangent function in Figure 4b (equation (3)) fit both the individual data points and the group averages (Figures 4b and 4d, $r^2 = 0.40$ and 0.63, respectively):

$$RNO_x = 15\ 2 + (35.5\text{atan}(0.68\pi(10D/D_o - 1.86)))/\pi, \quad (5)$$

where RNO_x = the ratio of NO_x to N_2O fluxes and D/D_o is the soil gas diffusivity.

2.5. NO_x Gas Submodel

NO_x emissions from soils are calculated as a function of the simulated N_2O flux, the NO_x:N_2O function, and a factor to account for pulses in NO_x emissions initiated by precipitation events. Total N_2O flux from nitrification and denitrification and the NO_x:N_2O function are used to calculate a base NO_x emission rate according to (6).

$$NO_x = RNO_x * N_2O_{den} + RNO_x * N_2O_{nit} * P. \quad (6)$$

NO_x is the potential soil gas flux of NO_x in gN ha^{-1} d^{-1}, RNO_x is the ratio of NO_x to N_2O gases emitted, N_2O_{den} is the simulated N_2O flux (gN ha^{-1} d^{-1}) from denitrification, N_2O_{nit} is the simulated N_2O flux from nitrification (gN ha^{-1} d^{-1}), and P is a pulse multiplier. We assume that no NO_x is emitted when the ground is covered with snow and that P=1 except during pulse episodes. The calculated potential NO_x flux is adjusted downward on days when the simulated NH_4^+ pool is not large enough to supply the N required to support the potential NO_x emission rate. The base NO_x flux associated with nitrification is modified to simulate the rapid rise in NO_x flux following rain onto a previously dry soil, independent of other controlling factors [*Smart et al.*, 1999; *Martin et al.*, 1998; *Hutchinson et al.*, 1993]. The submodel described by *Yienger*

and Levy [1995] was used to simulate the rapid rise in NO_x flux following such precipitation events. *Yienger and Levy* [1995] operationally define a soil as dry if it received less than 1 cm of precipitation during the previous 2 weeks. The magnitude and duration of the pulse are functions of the amount of precipitation received and the number of days since the event: If 0.1cm < precipitation < 0.5cm, then $P = 11.19e^{-0.805day}$, where 1 < day < 3; if 0.5cm < precipitation < 1.5cm, then $P = 14.68e^{-0.384day}$, where 1 < day < 7; if precipitation > 1.5cm, then $P = 18.46e^{-0.208day}$, where 1 < day < 14.

3. Data Sources

Most of the data used for model development were obtained from the U.S. Trace Gas Network (TRAGNET). TRAGNET was established in 1992 with the goals of documenting contemporary fluxes of CO_2, CH_4, N_2O, and NO_x and determining the major controls on trace gas flows. A long-term data archive is maintained to facilitate data comparisons and model building (http://www.nrel.colostate.edu/PROGRAMS/ATMOSPHERE/TRAGNET/TRAGNET.html).

The data sets used for model validation in this paper are located on the CENTURY web site (http://nrel.colostate.edu/PROGRAMS/MODELING/CENTURY/CENTURY.html) and include weekly soil water, temperature, NH_4^+, and NO_3^- and trace gas fluxes for N_2O and NO_x at different grassland sites and all of the data needed to run the trace gas ecosystem model (i.e., soil texture information, daily climate data, description of management practices, etc.). This data set is designed to test trace gas models and is particularly important since *Frolking et al.* [1998] showed that different trace gas models frequently predicted similar values for the N_2O fluxes but radically different values for the NO_x gas fluxes.

4. Model Testing

The DAYCENT model was tested by comparing simulated and observed daily soil water, NO_3^-, NH_4^+, and soil temperature and NO_x and N_2O flux data from five different short grass steppe sites in northeast Colorado. These sites included a fertilized (ammonium nitrate) and unfertilized pasture with a sandy loam texture (SLF and SL), a fertilized (urea) and unfertilized sandy clay loam site (SCLF and SCL), and a clay loam site (CL). The observed data for the soil variables and N_2O fluxes were collected weekly from 1990 to 1997 for the sandy loam and sandy clay loam sites, and from 1995 to 1997 at the clay loam site [*Mosier et al*, 1996; A. R. Mosier, unpublished data, 1995 to 1997]. At the time of gas flux sampling soil temperature was measured at 5 cm depth, soils (0-15 cm) were also analyzed gravimetrically to determine water content, and KCl extraction was used to infer soil NO_3^- and NH_4^+ concentrations (0-15 cm). N_2O flux was calculated based on the change in gas concentration at 0, 15, and 30 min. intervals after closed, vented chambers [*Hutchinson and Mosier*, 1981] were placed on permanent cylindrical anchors in field plots. Details of the gas sampling and analyses are given by *Mosier et al.* [1991, 1993]. The NO_x flux data were collected weekly or biweekly from 1994 to 1997 [*Martin et al.* 1998; A. R. Mosier, unpublished data, 1995 to 1997] by using a flow-through chamber method [*Slemr and Seiler*, 1984]. The chambers were placed on permanent anchors and changes in the NO_x concentration within the chambers were noted between 2 and 8 min. after the chambers were placed on the anchors. Changes in NO_x concentration were used to calculate NO_x flux according equations described by *Martin et al.* [1998]. Daily N_2O and NO_x flux measurements from four or six locations in each plot were used as replicates in statistical analysis.

The observed soil water, temperature, NO_3^-, and NH_4^+ data were not used to develop the model and can be considered a validation test of the model. The observed N_2O flux data from 1990 to 1993 were used in the development of N_2O trace gas flux model, while data collected after 1994 were used to validate and test the model. The individual NO_x flux observations were not used to parameterize the model, but the observed ratio of NO_x to N_2O fluxes were used to develop the NO_x:N_2O function (see NO_x:N_2O Data Analysis section).

In addition to comparing the model results with observed data, we wanted to evaluate how well our model was able to capture the overall patterns of NO_x and N_2O fluxes compared to existing models and statistical approaches. DAYCENT model results were compared to the *Yienger and Levy* [1995] NO_x flux model, a statistical NO_x model derived from the observed data, and the *Parton et al.* [1988] N_2O flux model. The comparison of DAYCENT model results with the observed data is designed to show how well the model simulates day-to-day changes in the soil variables, trace gas fluxes, the seasonal patterns in the observed variables, and the impact of soil texture and fertility on mean annual trace gas fluxes.

5. Model Versus Data Comparison

5.1. Soil Water Content and Temperature

The comparison of simulated versus observed water-filled pore space (WFPS 0-15 cm depth) for April through October (Figure 5a) shows that the model simulates soil water content well during the growing season for all of the sites ($r^2 = 0.64$). However, the modeled soil water content was inadequate during the nongrowing season (Figure 5b, $r^2 = 0.27$ for November- March). The lack of fit is probably a result of microscale patterns in snow distribution associated with snow drifting, which is represented in the six, 2.5 cm soil samples which were pooled for each measurement, but is not adequately represented in the model. Although the model did well when judged with the r^2 criterion, the model was biased in that simulated summer WFPS values tended to be overestimated (Figure 5a). Figure 5c shows the tendency of the model to overestimate summer WFPS and the failure of the model to capture winter season WFPS dynamics in the beginning of the year. Overall, this limited comparison is consistent with other comparisons which demonstrate the ability of DAYCENT to simulate soil water dynamics and daily actual evapotranspiration rates across a wider range of sites [*Parton et al.*, 1998].

Modeled and observed soil temperature at 5 cm soil depth compare favorably ($r^2 = 0.79$) at the time of the trace gas flux observation (10:00 A.M.-12:00 noon, MST), and DAYCENT adequately captures the average annual seasonal cycle (Fig7re 6). Again this limited comparison of modeled and observed soil temperatures is consistent with comparisons across a broader range of sites [*Eitzinger et al.*, 2001; *Parton et al.*,

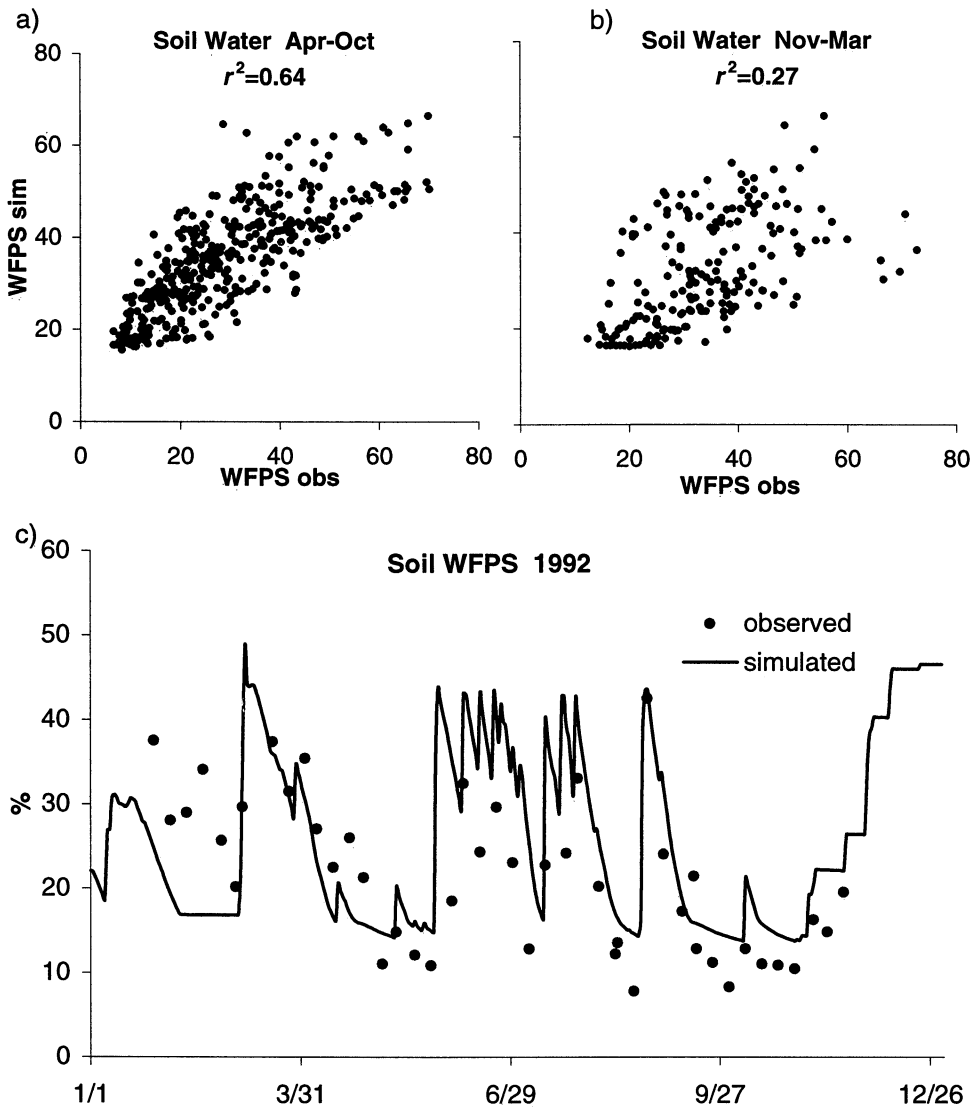

Figure 5. Comparison of simulated versus measured soil water-filled pore space (WFPS) for all the sites (a) during the growing season and (b) during the winter months. (c) Daily comparison of simulated and observed WFPS for the sandy loam site during 1992.

1998]. Overall, with the exception of the winter soil water dynamics, the DAYCENT model simulates well the soil water and temperature parameters that are used as inputs into the trace gas flux submodel (Figures 5 and 6).

5.2. Soil NH_4^+ and NO_3^- Concentrations

The comparison of observed versus simulated soil NH_4^+ and NO_3^- concentrations is limited by the representativeness of the samples and concentrations near the detection limit. Measurements of soil NO_3^- and NH_4^+ are spatially and temporally variable. Long-term experiments require a small number of soil samples (four or six, 2.5 cm cores were collected for each observation) on any given sample date with the number of samples being inadequate to represent NO_3^- and NH_4^+ levels at the sites. These aspects make it extremely hard to correctly characterize the mineral N concentration and lead to the model versus data comparison presented here. Because of the limitations involved with the daily mineral N measurements, we calculated site and seasonal averages for observed and simulated total mineral N (NO_3^- + NH_4^+). For this analysis we defined seasons as winter (December-February), spring (March-May), summer (June-August), and autumn (September-November). The model underestimated mineral N concentrations in all of the soils but correctly simulated higher mineral N values in the SLF soil compared to the native SL soil. However, the model simulated higher values in the SCLF compared to the native SCL, but the data showed no significant differences in the mineral N concentrations of these soils. The model and data both showed lower mineral N values in the native coarse-textured (SL) soil than the native medium-textured (SCL) soil. The comparison of observed versus simulated seasonal averages of NH_4^+ + NO_3^- for the different sites showed that the model correctly simulated the observed pattern of higher mineral N levels during the winter and early spring and low mineral 8l values during the summer and autumn. However, seasonality was better simulated in the SCL and SCLF (r^2 = 0.79 and r^2 = 0.81, respectively) compared to the SL and SLF sites (r^2 =

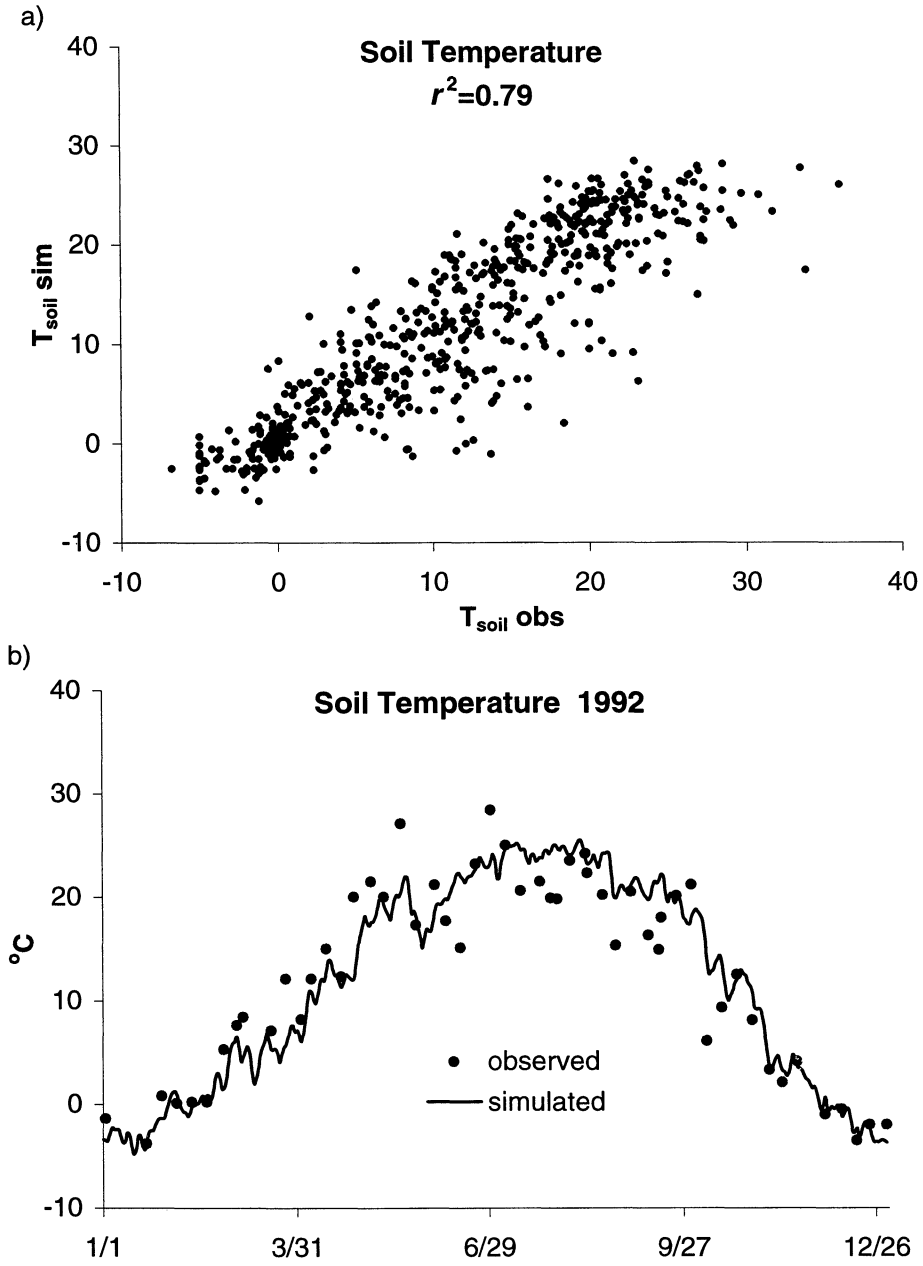

Figure 6. Comparison of simulated (daily average at 15 cm depth) versus measured (10am to12 noon) soil temperature (a) for all the sites and (b) daily comparison of simulated and observed soil temperature for the sandy loam site during 1992.

0.65 and r^2 = 0.57, respectively). Observed mineral N data were not available for the CL soil.

5.3. Soil N_2O and NO_x Fluxes

The annual average observed N_2O and NO_x fluxes are close to the simulated values across the range of soil textures and fertilizer treatments (Figure 7). Observations showed that the N_2O fluxes are higher in the fertilized sandy loam (SLF) and fertilized sandy clay loam (SCLF) compared to the native sandy loam (SL) and native (SCL) soils and that N_2O emissions are highest from the clay loam (CL), intermediate for the sandy clay loam (SCL), and lowest for the sandy loam (SL). The model generally showed the same patterns, except that N_2O emissions were somewhat underestimated for the CL soil. Observations showed that NO_x fluxes are enhanced for the fertilized sandy loam site and decrease as the clay content of the soil increases (clay content increases along the gradient from sandy loam, to sandy clay loam, to clay loam sites). However, the model incorrectly simulated higher NO_x emissions from the SCLF site compared to the SCL site and incorrectly simulated essentially equivalent NO_x emissions from the SCL and Cl soils.

Statistical analyses were performed to evaluate how well DAYCENT simulated the observed daily and seasonal patterns of N gas fluxes (Table 1). The model simulated N_2O and NO_x fluxes better during the growing season (April-

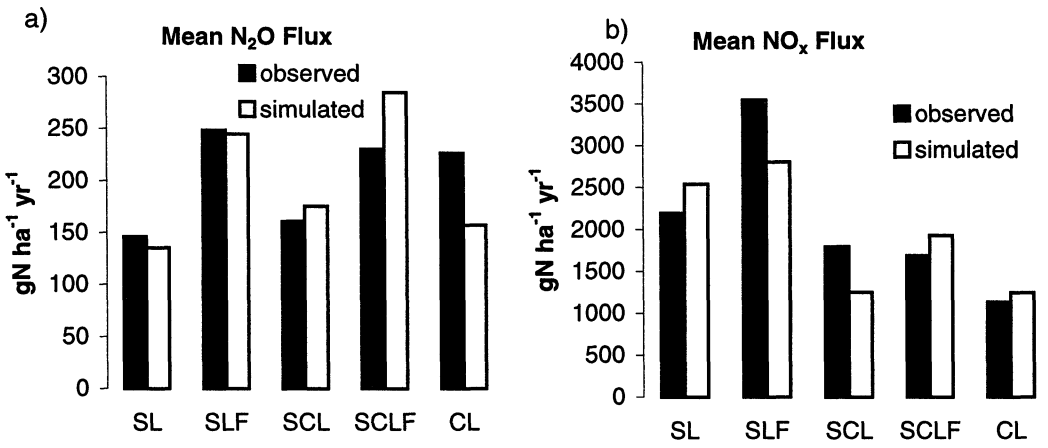

Figure 7. Comparison of observed and simulated mean annual (a) N_2O and (b) NO_x gas flux rates for the five grassland sites. SL, sandy loam; SLF, sandy loam fertilized; SCL, sandy clay loam; SCLF, sandy clay loam fertilized; CL, clay loam.

October) than during the nongrowing season (November-March). Table 1 also shows that r^2 values for N_2O during both seasons and NO_x during the nongrowing season tend to be higher when calculated at the monthly compared to the daily timescale while the opposite trend exits with NO_x during the growing season. The model fits the data better at the monthly timescale for N_2O because N_2O emission events are often mistimed by a few days or more and daily inconsistencies are not important at the monthly timescale. DAYCENT does better simulating growing season NO_x fluxes at the daily timescale because the large NO_x emissions are highly event driven. The *Yienger and Levy* [1995] pulse multiplier used by DAYCENT predicts elevated NO_x emissions on the day of certain nonsnow precipitation events and for succeeding days for up to 2 weeks. Consequently, the model does well on a daily basis during the growing season because the importance of timing events exactly is diminished. Monthly r^2 values are lower because the importance of sporadic NO_x emission episodes, to which the model is sensitive, is diminished.

Figure 8 shows observed and simulated average monthly N_2O and NO_x emissions. Simulated N_2O emissions are due almost exclusively to nitrification during the growing season while denitrification makes a significant contribution during the winter and spring (Figures 8a, 8c and 8e). The comparison of simulated and observed monthly average N_2O flux rates (Figures 8a, 8c and 8e) and statistics (Table 1) shows that the model simulates seasonality well in the coarse-textured pasture sites (SL and SLF) and in the finer-textured site (CL), but that seasonality is poorly simulated for the SCL and the SCLF sites. The SCL and SCLF sites are located in a low-lying swale, which may explain the anomalous results for these soils. For the nonswale sites, observations show that fluxes are highest in summer, lower in the spring and fall months, and that there is a secondary peak in N_2O flux during the winter season. However, the observed data for the swale sites show little evidence of a strong seasonal pattern. Winter season fluxes are enhanced and summer season fluxes depressed compared to the other sites. Nutrient deposition and

Table 1. Correlation Coefficient (r^2), p Value (p), and Slope (m) Statistics for the Linear Regression of Observed Versus Simulated N Gas Fluxes

	Daily Statistics						Monthly Statistics		
	Growing Season			Nongrowing Season			Year-Round		
Soil	r^2	p	m	r^2	p	m	r^2	p	m
				N_2O					
SL	0.07	0.0001	0.16	0.00	0.74	-0.05	0.35	0 045	0 41
SLF	0.19	0.0001	0.23	0.04	0.015	0.53	0.46	0.16	0.65
SCL	0.08	0.0006	0 24	0 00	0.36	-0.07	0.18	0.19	-0 16
SCLF	0.02	0 14	0.01	0.01	0.29	-0.24	0.02	0.69	0.07
CL	0.02	0.10	0.36	0 04	0.15	0.22	0.64	0.01	0.68
Overall	0 09	0.0001	0 12	0 00	0.305	0.10	0.26	0.0001	0.38
				NO_x					
SL	0.63	0 0001	0.79	0 21	0.005	0.84	0.76	0.0002	0.73
SLF	0.41	0.0001	1.1	0.24	0.0027	0.98	0.21	0.14	0.40
SCL	0 07	0.20	0.20	0.04	0.27	1.48	0.00	0.95	-0.02
SCLF	0.17	0.095	0.72	0.24	0.0057	0.88	0.27	0.08	0.57
CL	0 69	0.0001	0.61	0.11	0.17	2.4	0.20	0.13	0.61
Overall	0.50	0.0001	0.86	0.12	0.001	0.94	0.27	0.0001	0.48

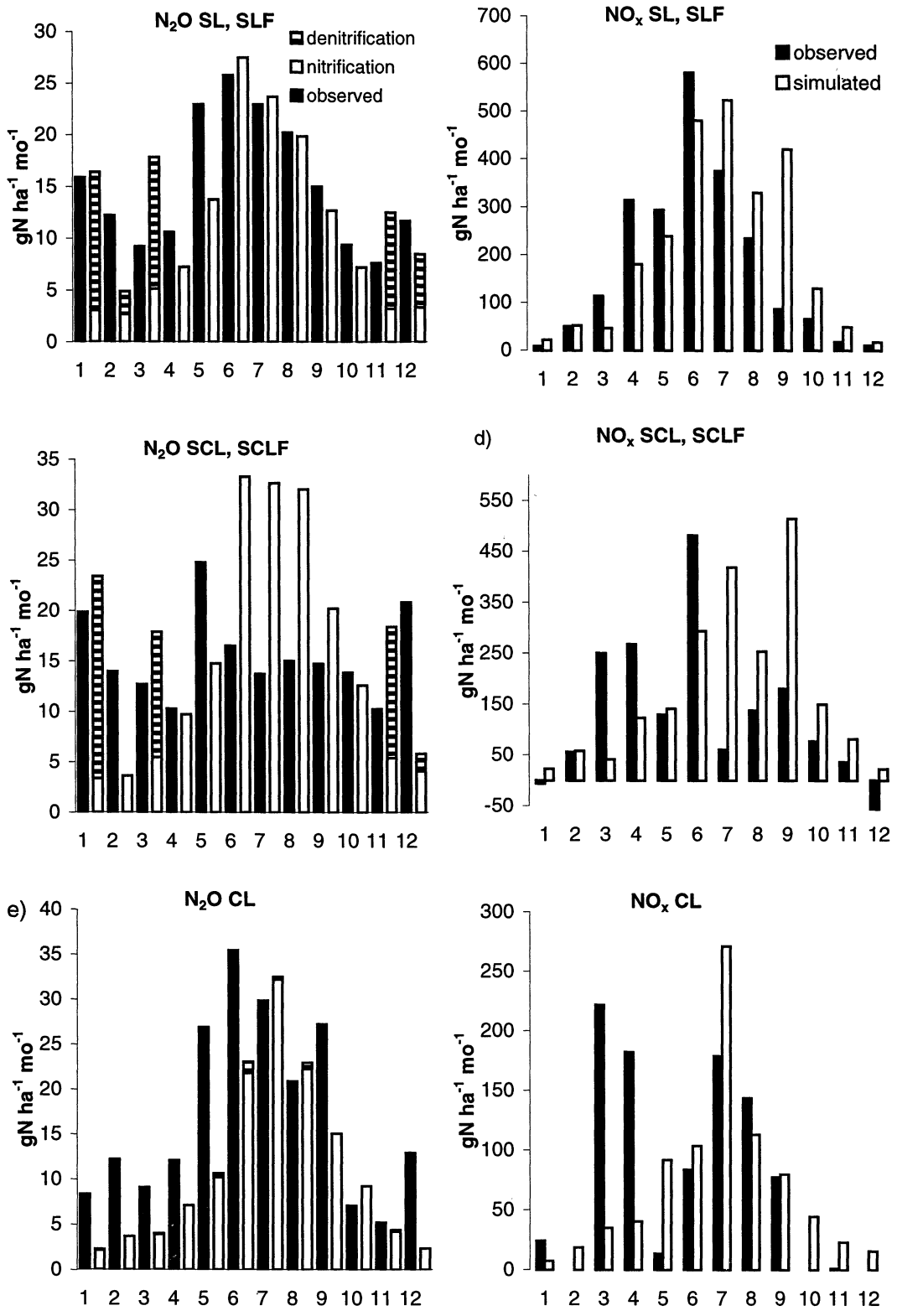

Figure 8. Comparison of observed and simulated mean monthly N_2O and NO_x flux rates for (a,b) sandy loam (SL) and sandy loam fertilized (SLF), (c,d) sandy clay loam (SCL) and sandy clay loam fertilized (SCLF), and (e,f) clay loam (CL) grassland soils. Simulated N_2O emissions bars show the amount of total N_2O emissions that are due to nitrification and denitrification.

a different plant community in the swale may be responsible for the seasonal pattern of the observed N_2O fluxes for the SCL and SCLF sites.

The seasonal pattern of NO_x fluxes in the coarse textured (SL and SLF) soils was well simulated by DAYCENT (Figure 8b). However, for the finer textured soils (SCL, SCLF and CL) the model tended to underestimate NO_x fluxes during March and April (Figures 8d and 8f). The reason is unclear but is likely the result of underestimating nitrification rates during the early spring months. Both model results and data show little NO_x emissions during the winter, suggesting that N_2O fluxes in the summer are due primarily to nitrification while the observed winter season N_2O emissions are due to denitrification events. Although the model simulated low NO_x emission rates during winter, winter and autumn season NO_x fluxes were often overestimated (Figures 8b, 8d and 8f). The winter season, and to a lesser extent autumn season, overestimations are at least partially due to observed NO_x flux rates reflecting both uptake and emissions of NO_x by soils, whereas only NO_x emissions are simulated by the model. This is more of a problem during the winter because atmospheric concentrations of NO_x are high so NO_x diffuses into the soil at higher rates than during the summer.

Figure 9 shows the time series of simulated and observed N_2O fluxes for the SL soil. The high-observed average monthly N_2O fluxes during the winter months (Figures 8a, 8c and 8e) are caused by a small number of large fluxes (Figure 9). The variability in measured N_2O flux rates is substantial, and the number of days when the model results were within ±1 standard deviation of the observed data was 48% during the growing season (April-October) and 43% during the winter showing that model performance is similar during both seasons using this criterion. However, the model did better during the growing season from the r^2 criterion (Table 1). This same type of analysis has been run for other sites and shows similar results with large year-to-year and seasonal differences in model performance [*Frolking et al.*, 1998]. The version of the model used by *Frolking et al.* [1998] was biased in that winter season N_2O emissions were underestimated. The current version which includes the changes in the denitrification and snowmelt submodels described earlier is less biased during the winter, but r^2 values are still low. The low r^2 values when calculated on a daily basis result from the model's inability to properly time the occasional large flux events, especially during the winter. This is not surprising because the precipitation events in the data that are used to drive the model may be a day earlier or a day later than the actual events and water inputs from snowmelt events are influenced by topography and wind velocity which are not included in the model.

Simulated and observed NO_x fluxes have low values during the winter and high values during the spring and summer (Figure 10). Both model and observed data show large NO_x fluxes occur following rainfall onto dry soil which drives much of the day-to-day variability in NO_x fluxes. The model results generally represent the observed data fairly well for the sandy loam soil except when the model missed large NO_x fluxes. Similar comparisons of the DAYCENT model results with observed data from the other sites showed comparable results for all of the sites except the native sandy clay loam (SCL) where the model performed poorly (Table 1). The proportion of days when the model simulated NO_x flux within +/-1 standard deviation of the observed data for all of the sites was 52%.

6. DAYCENT Comparison With Alternative Models

This section compares the results of the DAYCENT N_2O and NO_x flux model with other trace gas models. Recent model comparison efforts have shown that the best way to evaluate model performance is to compare model results from different models with standard observed data sets. This approach has been used by *Ryan et al.* [1996] to compare forest growth models, by *Parton et al.* [1993] for grassland ecosystem models, by *Shao and Henderson-Sellers* [1996] for water flow models, and by *Frolking et al.* [1998] for N_2O trace gas flux models. *Frolking et al.* [1998] demonstrated that this is particularly appropriate for trace gas flux models since there are large spatial and temporal variations in the observed trace gas flux data that make it difficult to adequately evaluate trace gas models.

The DAYCENT NO_x flux results were compared with the *Yienger and Levy* [1995] global soil NO_x emission model and a statistical model. The *Yienger and Levy* [1995] model was parameterized with a global data set and simulates NO_x emissions as a function of soil water content, soil temperature, precipitation, biome type, fertilization rate, and accounts for NO_x uptake by the plant canopy as well as the effects of biomass burning. The *Yienger and Levy* [1995] model underestimated NO_x emissions from the soils used for model testing by values ranging from 28% to 80%. To compensate for this, we augmented the *Yienger and Levy* [1995] model with an optimized site multiplier for each soil to account for fertility and textural differences among the soils. The statistical model uses soil water and temperature equations and site factors for each soil that represent the soil texture and fertility differences (multiplication of site factor and the soil water and soil temperature equations). The best fitting NO_x regression model had an observed versus simulated $r^2 = 0.10$, while the modified *Yienger and Levy* [1995] model had an observed versus simulated $r^2 = 0.32$. DAYCENT performed somewhat better with an $r^2 = 0.43$ for all the sites combined. These results show that combining the *Yienger and Levy* [1995] rainfall event multipliers with the DAYCENT model which simulates NO_x fluxes as a function of N_2O fluxes and soil gas diffusivity results in a superior NO_x flux model and suggest that the rainfall event impact on NO_x fluxes explains a substantial part of the temporal variations in NO_x fluxes for these semiarid ecosystems. In other ecosystems where water is less limiting, the temporal dynamics are likely to be driven by other processes.

DAYCENT-simulated N_2O flux results were compared with the N_2O regression model developed by *Parton et al.* [1988] and modified to include site factors that represent soil specific texture and fertility differences (determined using nonlinear optimization to the observed N_2O flux data). The regression model combined observed versus simulated $r^2 =$ 0.06 and 0.18, respectively, for winter and the growing season, while the DAYCENT $r^2 = 0.0$ and 0.09, respectively. The results show that the regression model performs better than the DAYCENT model, both models perform better during the growing season, and both models show poor performance when evaluated with the r^2 criterion. One reε12n for the regression model doing better is that the regression model uses the measured soil WFPS and temperature to simulate N_2O emissions, whereas DAYCENT uses modeled values of these parameters to drive the N_2O flux submodel.

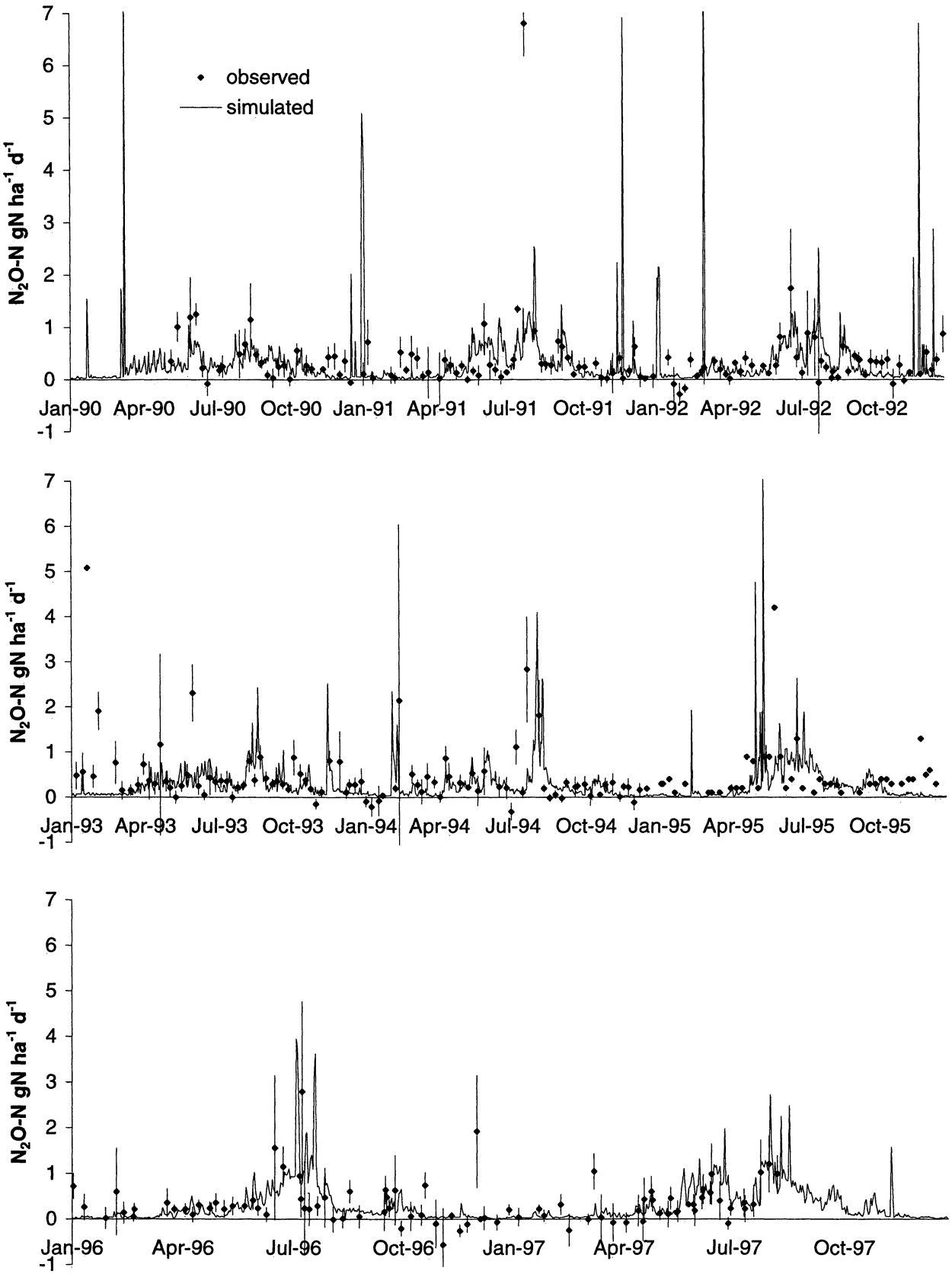

Figure 9. Comparison of observed and simulated daily N_2O fluxes for the native sandy loam site. Error bars represent standard deviations of measurement repetitions (n=4); standard deviations were not available for all measurements.

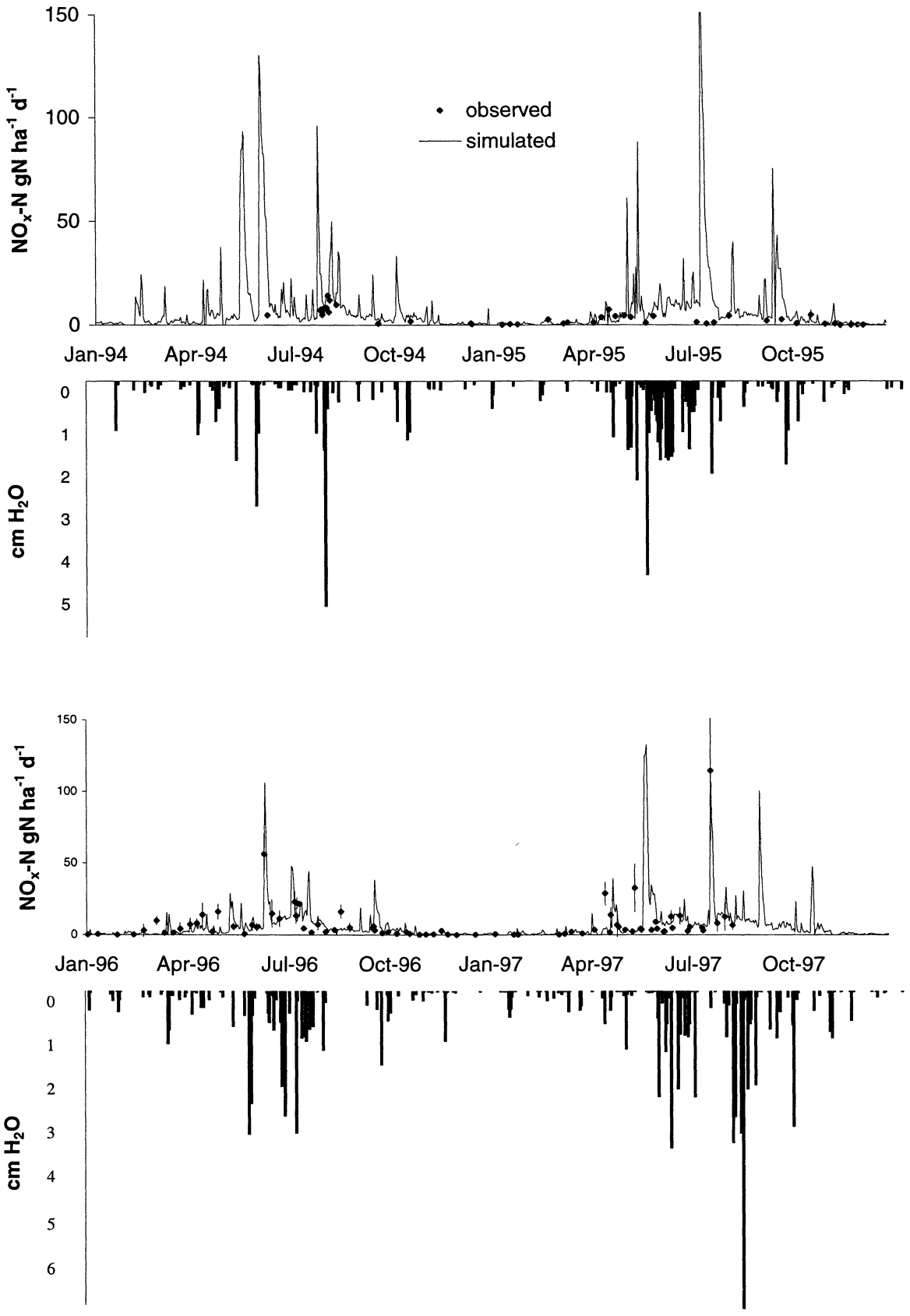

Figure 10. Comparison of observed and simulated daily NO_x fluxes for the native sandy loam soil with daily precipitation amounts. Error bars represent standard deviations of measurement repetitions (n=4); standard deviations were not available for all measurements.

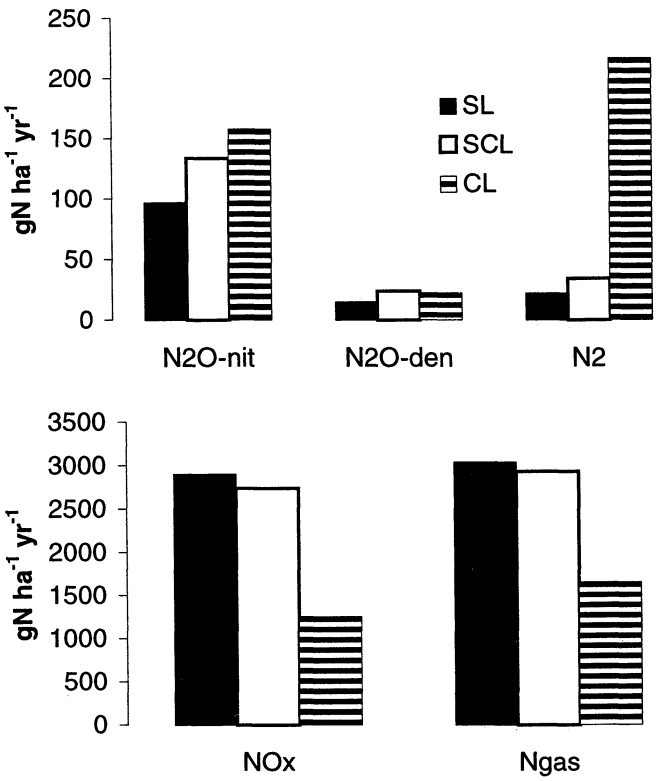

Figure 11. Sensitivity to soil texture of simulated N_2O flux from nitrification, N_2O flux from denitrification, N_2 flux from denitrification, NO_x from nitrification and denitrification, and total N gas flux.

7. N Gas Submodel Sensitivity Analysis

To compare the effects of soil physical properties on N gas emissions, we calculated average annual N_2O emissions from nitrification, N_2O emissions from denitrification, N_2 emissions from denitrification, NO_x emissions from nitrification and denitrification, and total N gas emissions for the native soils used for model validation (Figure 11). N_2O emissions from nitrification increased as soils became finer textured because simulated mineral N levels increased as soils became finer in texture. N_2O emissions from denitrification were lowest for the sandy loam soil because the anaerobic conditions that facilitate denitrification are less likely to develop in sandy soils that drain readily. N_2 emissions from denitrification increased as soils became finer textured. This is driven by the decrease in soil gas diffusivity associated with higher water retention and a larger proportion of micropores in fine-textured soils. Lower gas diffusivity is assumed to result in an increase in anoxic microsites and increase the probability that N_2O from denitrification will be further reduced to N_2 before diffusing from the soil. For similar reasons, NO_x emissions decreased as soils became finer textured. The NO_x:N_2O function is used to indicate the relative proportions of N gas flux that are due to nitrification and denitrification. The model assumes that NO_x:N_2O is higher for nitrification than for denitrification and that a higher proportion of total N gas flux is due to denitrification as soil gas diffusivity decreases. Total N gas emissions tended to decrease as soils became finer textured due to the associated decrease in simulated NO_x emissions.

8. Summary

This paper provides a detailed description and testing of a new submodel to simulate NO_x fluxes and an updated submodel for simulating nitrification and N_2O gas fluxes associated with nitrification. As part of the development of the NO_x flux model, we analyzed NO_x flux data from 10 sites around the world and developed an equation for predicting the ratio of NO_x to N_2O fluxes as a function of soil gas diffusivity. We demonstrated that this is an improvement over existing models [*Verchot et al.*, 1999; *Davidson and Verchot*, 2000] that simulate NO_x:N_2O as a function of water-filled pore space. The NO_x:N_2O function is based on the following assumptions: nitrification has a higher NO_x:N_2O than denitrification, and soil gas diffusivity is correlated with the relative contributions of nitrification and denitrification to total N gas emissions. There is considerable variability in NO_x:N_2O that is not explained as function of WFPS or soil diffusivity and is most likely associated with the large increase in NO_x fluxes following rainfall events when the soil has been dry prior to the rainfall event [*Smart et al.*, 1999; *Martin et al.*, 1998; *Yienger and Levy*, 1995; *Hutchinson et al.*, 1993]. The detailed testing of the DAYCENT NO_x flux submodel has demonstrated that adding the *Yienger and Levy* [1995] rainfall event multipliers for NO_x fluxes greatly improved the ability to simulate NO_x fluxes for a variety of grassland sites. It suggests that most of the day-to-day changes in NO_x fluxes for these sites are controlled by the rainfall event multipliers that are a function of rainfall amount, time since rainfall, and the length of dry period prior to the rainfall event.

The ability of DAYCENT to simulate the dynamics of soil nutrients, soil water and temperature, and soil NO_x and N_2O trace gas fluxes was evaluated using an extensive observed data set for five different grassland sites which included different soil textures and soil fertility levels measured from 1990 to 1997. DAYCENT adequately simulated the day-to-day variations and seasonal changes in soil temperature. DAYCENT simulated soil water dynamics well during the growing season, but the dynamics were not well represented during the winter months. We think that spatial variations in snow cover due to extensive snow drifting are the major cause for this problem. DAYCENT simulation of soil mineral N ($NH_4^+ + NO_3^-$) concentrations compared reasonably well with the observed seasonal patterns and differences in site fertility levels with both the data and model, although soil mineral N levels were consistently underestimated by the model. Mineral N levels were highest during the winter and spring and low during the summer, and the N fertilized sites had higher mineral N levels. DAYCENT correctly simulated the observed seasonal patterns of NO_x fluxes (high fluxes during the summer and low fluxes during the winter), the major differences in annual NO_x flux among the different sites (higher fluxes with sandy soils as compared to fine textured soils), and the day-to-day variations in NO_x fluxes in response to soil water, temperature, and rainfall events. The major discrepancy noted in the model versus data comparison was a tendency to underestimate NO_x gas fluxes during the spring. The error may be related to the limited ability to predict ammonium dynamics at the level experienced by the nitrifying organisms.

DAYCENT simulated N_2O fluxes show that the model correctly simulated the observed seasonal pattern of low N_2O

fluxes during the winter and high fluxes during the summer (except for the SCL and SCLF soils) and the elevated N_2O fluxes associated with adding nitrogen fertilizer. The observed mean seasonal pattern in N_2O flux shows a secondary peak in N_2O fluxes during the winter. A detailed analysis of the observed data showed that generally, several large fluxes associated with apparent denitrification events drive the average flux to be relatively high during the winter, while most of the winter N_2O fluxes are low. The exception is the two soils (SCL and SCLF) that are located in a low-lying swale. The swale is in a depositional zone that receives higher inputs then the other sites, and, consequently, has higher productivity and a different plant community. DAYCENT does not include effects of topography on nutrient and water availability which may explain why N_2O emissions from the SCL and SCLF soils were simulated poorly, although mineral N concentrations were modeled fairly well in these soils. We believe that the higher winter N_2O fluxes emitted from the swale soils are a result of higher fertility levels, but the reasons for the relatively low summer N_2O values for these soils (Figure 8c) remain unclear. We speculate that the lack of high summer fluxes in the observed data for the swale soils reflects controls on the processes that we do not understand or that the key processes are influenced to a greater extent in these soils by smaller scale variations in the drivers than are resolved by the model.

Acknowledgments. The research for this paper was supported by the National Aeronautics and Space Administration, the National Science Foundation, the Department of Energy, and the Environmental Protection Agency through the following grants: NASA-EOS NAGW 2662, NSF-LTER BSR9011659, DOE NIGEC LWT62-123-06516, and EPA Regional Assessment R824939-01-0. The authors also wish to thank two anonymous reviewers whose suggestions greatly increased the accuracy and clarity of this paper.

References

Brasseur, G.P., J.J. Orlando, and G.S. Tyndall (Eds), *Atmospheric Chemistry and Global Change*, Oxford Univ. Press, New York, 1999.

Chameides, W.L., P.S. Kasibhatla, J. Yienger, and H Levy II, Growth of continental scale metro-agro-plexes, regional ozone pollution, and world food production, *Science, 264*, 74-77, 1994

Conrad, R., Soil microorganisms as controllers of atmospheric trace gases (H_2, CO, CH_4, OCS, N_2O, and NO), *Microbiol. Rev., 60*, 609-640, 1996.

Davidson, E.A , Fluxes of nitrous oxide and nitric oxide from terrestrial ecosystems, in *Microbial Production and Consumption of Greenhouse Gases: Methane, Nitrogen Oxides, and Halomethanes*, edited by J.E. Rogers and W.B. Whitman, pp. 219-235, Am Soc. for Microbiol., Washington, D. C., 1991.

Davidson, E.A., Soil water content and the ratio of nitrous oxide to nitric oxide emitted from soil, in *Biogeochemistry of Global Change: Radiatively Active Trace Gases*, edited by R.S Oremland, pp. 369-386, Chapman and Hall, New York, 1993.

Davidson, E.A., and W. Kingerlee, A global inventory of nitric oxide emissions from soils, *Nutr. Cycling Agroecosyst., 48*, 37-50, 1997

Davidson, E.A., and L.V. Verchot, Testing the hole-in-the-pipe model of nitric and nitrous oxide emissions from soils using the TRAGNET data base, *Global Biogeochem. Cycles, 14*, 1035-1043, 2000.

De Groot, C J., A. Vermoesen, and O. Van Cleemput, Laboratory study of the emission of NO and N_2O from some Belgian soils, *Environ. Monit. Assess., 31*, 183-189, 1994.

Del Grosso, S.J., W.J. Parton, A.R. Mosier, M.D. Hartman, J. Brenner, D.S. Ojima, and D.S. Schimel, Simulated interaction of carbon dynamics and nitrogen trace gas fluxes using the DAYCENT model, in *Modeling Carbon and Nitrogen Dynamics for Soil Management*, edited by M. Shaffer, S. Hansen, and L. Ma, pp. 303-332, CRC Press, Boca Raton, Florida, 2001.

Del Grosso, S J., W.J. Parton, A.R. Mosier, D.S. Ojima, A.E. Kulmala, and S Phongpan, General model for N_2O and N_2 gas emissions from soils due to denitrification, *Global Biogeochem. Cycles, 14*, 1045-1060, 2000.

Delmas, R , D. Serca, and C. Jambert, Global inventory of NO_x sources, *Nutr Cycling Agroecosyst., 48*, 51-60, 1997.

Doran, J W , L N Mielke, and S. Stramatiadis, Microbial activity and N cycling as regulated by soil water-filled pore space, paper presented at 11th International Conference, Int. Soil Tillage Res. Org (ISTRO), Edinburgh, Scotland, 1988.

Eitzinger, J , W J. Parton, and M.D Hartman, Improvement and validation of a daily soil temperature submodel for freezing/thawing periods, *Soil Sci 165*, 525-534, 2001

Ellis, S., K Goulging, and L Dendooven, Effect of pH on nitrous oxide emissions from grassland soil, in *Gaseous Nitrogen Emissions From Grasslands*, edited by S.C. Jarvis and B F. Pain, pp. 181-188, CAB International, Wallingford, England, 1997.

Firestone, M K , and E.A Davidson, Microbial basis of NO and N_2O production and consumption in soils, in *Exchange of Trace Gases Between Terrestrial Ecosystems and the Atmosphere*, edited by M.O Andreae and D S. Schimel, pp. 7-21, John Wiley, New York, 1989

Frolking, S E., et al , Comparison of N_2O emissions from soils at three temperate agricultural sites: Simulations of year round measurements by four models, *Nutr. Cycling Agroecosyst., 52*, 77-105, 1998.

Gasche, R., and H. Papen, A 3-year continuous record of nitrogen trace gas fluxes from untreated and limed soil of a N-saturated spruce and beech forest ecosystem in Germany, 2, NO and NO_2 fluxes, *J. Geophys Res., 104*, 18,505-18,520, 1999.

Grant, R.F., and E Pattey, Mathematical modeling of nitrous oxide emissions from an agricultural field during spring thaw, *Global Boigeochem Cycles, 13*, 679-694, 1999.

Hauglustaine, D A. G.P Brasseur, S. Walters, P.J. Rasch, J F Müller, L.K. Emmons, and M.A. Carroll, MOZART, a global chemical transport model for ozone and related chemical tracers, 2, Model results and evaluation, *J. Geophys. Res., 103*, 28,291-28,335, 1998

Hauglustaine, D.A G.P. Brasseur, and J.S. Levine, A sensitivity simulation of tropospheric ozone changes due to the 1997 Indonesian fire emissions, *Geophys. Res. Lett., 26*, 3305-3308, 1999.

Holland, E.A., and J.F Lamarque, Modeling bio-atmospheric coupling of the nitrogen cycle through NO_X emissions and NO_Y deposition, *Nutr. Cycling Agroecosys., 48*, 7-24, 1997.

Holland, E.A , F.J Dentener, B H. Braswell, and J.M. Sulzman, Contemporary and pre-industrial reactive nitrogen budgets, *Biogeochemistry, 46*, 7-43, 1999.

Howarth, R.W., et al., Regional nitrogen budgets and riverine N and P fluxes for the drainages to the North Atlantic Ocean: Natural and human influences, *Biogeochemistry, 35*, 75-139, 1996.

Hutchinson, G.L , and A.R Mosier, Improved soil cover method for field measurement of nitrous oxide fluxes, *Soil Sci. Soc. Am. J., 45*, 311-316, 1981

Hutchinson, G.L., G.P. Livingston, and E.A. Brams, Nitric and nitrous oxide evolution from managed subtropical grassland, in *Biogeochemistry of Global Change: Radiatively Active Trace Gases,* edited by R.S. Oremland, pp. 290-316, Chapman and Hall, New York, 1993

Keller, M., E. Veldkamp, E. Weitz, and W.A. Reiners, Pasture age effects on soil-atmsophere trace gas exchange in a deforested area of Costa Rica, *Nature, 365*, 244-246, 1993.

Kelly, R.H , W J. Parton, M.D. Hartman, L K. Stretch, D.S. Ojima, and D.S Schimel, Intra and interannual variability of ecosystem processes in shortgrass steppe, *J. Geophys. Res., 105*, 20,093-20,100, 2000.

Kroeze, C , A. Mosier, and L Bouwman, Closing the global N_2O budget: A retrospective analysis 1500-1994, *Global Biogeochem. Cycles, 13*, 1-8, 1999.

Lee, D.S., I. Köhler, E. Grobler, F. Rohrer, R. Sausen, L. Gallardo-Klenner, J.G. Oliver, F.J. Dentener, and A.F. Bowman, Estimates of global NO_x emissions and their uncertainties, *Atmos. Environ., 31*, 1735-1749, 1997.

Levy, H. II, P.S Kasibhatla, W.J Moxim, A.A. Klonecki, A.I. Hirsch, S.J. Oltmans, and W.L. Chameides, The global impact of human activity on tropospheric ozone, *Geophys. Res. Lett., 24*, 791-794, 1997.

Li, C , S. Frolking, and T.A. Frolking, A model of nitrous oxide

evolution from soil driven by rainfall events, 1, Model structure and sensitivity, *J Geophys Res*, *97*, 9777-9796, 1992

Li, C, J Aber, F Stange, K Butterbach-Bahl, and H. Papen, A process-oriented model of N_2O and NO emissions from forest soils, 1, Model development, *J Geophys Res*, *105*, 4369-4384, 2000

Linn, D M, and J.W Doran, Effect of water-filled pore space on carbon dioxide and nitrous oxide production in tilled and nontilled soils, *Soil Sci Soc Am J*, *48*, 1267-1272, 1984

Madronich, S., and P Hess, The oxidizing capacity of the troposphere and its changes, in *Proceedings of the Sixth European Symposium on the Physico-chemical Behavior of Atmospheric Pollutants*, October 18-22 1993, vol 1, pp 5-13, Commission of the European Communities, Varese, Italy, 1994

Malhi, S.S., and W B. McGill, Nitrification in three Alberta soils: Effect of temperature, moisture, and substrate concentration, *Soil Biol Biohcem*, *14*, 393-399, 1982

Martin, R E, M C Scholes, A R. Mosier, D S Ojima, E A Holland, and W J Parton, Controls on annual emissions of nitric oxide from soils of the Colorado shortgrass steppe, *Global Biogeochem. Cycles, 12*, 81-91, 1998.

Matson, P A, R Naylor, and I Ortiz-Monasterio, Integration of environmental, agronomic, and economic aspects of fertilizer management, *Science, 280*, 112-115, 1998

Millington, R J, and R C Shearer, Diffusion in aggregated porous media, *Soil Sci*, *111*, 372-378, 1971.

Mosier, A.R., D S Schimel, D W Valentine, K F Bronson, and W J Parton, Methane and nitrous oxide fluxes in native, fertilized, and cultivated grasslands, *Nature, 350*, 330-332, 1991.

Mosier, A R, D W Valentine, D S Schimel, W J Parton, and D S Ojima, Methane consumption in the Colorado shortgrass steppe, *Mitt. Dtsch Bodenk. Ges., 69*, 219-226, 1993.

Mosier, A.R., W J Parton, D W Valentine, D S Ojima, D S. Schimel, and J A Delgado, CH_4 and N_2O fluxes in the Colorado shortgrass steppe, 1, Impact of landscape and nitrogen addition, *Global Biogeochem Cycles, 10*, 387-399, 1996.

Mosier, A R, W J Parton, D.W Valentine, D S Ojima, D S. Schimel, and O Hienemeyer, CH_4 and N_2O fluxes in the Colorado shortgrass steppe, 2, Long-term impact of land use change, *Global Biogeochem Cycles, 11*, 29-42, 1997

Mosier, A., C Kroeze, C. Nevison, O. Oenema, S Seitzinger, and O van Cleemput, Closing the global N_2O budget: Nitrous oxide emissions through the agricultural nitrogen cycle, *Nutr Cycling Agroecosyst., 52*, 225-248, 1998.

Papen, H, and K Butterbach-Bahl, A 3-year continuous record of nitrogen trace gas fluxes from untreated and limed soil of a N-saturated spruce and beech forest ecosystem in Germany, 1, N_2O emissions, *J Geophys. Res*, *104*, 18,487-18,503, 1999

Parton, W.J., A R. Mosier, and D.S. Schimel, Rates and pathways of nitrous oxide production in a shortgrass steppe, *Biogeochemistry, 6*, 45-58, 1988

Parton, W J, et al, Observations and modeling of biomass and soil organic matter dynamics for the grassland biome worldwide, *Global Biogeochem. Cycles, 7*, 785-809, 1993.

Parton, W.J., A R. Mosier, D.S Ojima, D W. Valentine, D.S. Schimel, K Weier, and K E Kulmala, Generalized model for N_2 and N_2O production from nitrification and denitrification, *Global Biogeochem Cycles, 10*, 401-412, 1996.

Parton, W.J, M Hartman, D S Ojima, and D S. Schimel, DAYCENT: Its land surface submodel: Description and testing, *Global Planet Change, 19*, 35-48, 1998.

Potter, C S., P A Matson, P.M Vitousek, and E.A. Davidson, Process modeling of controls on nitrogen trace gas emissions from soils worldwide, *J. Geophys. Res*, *101*, 1361-1377, 1996a.

Potter, C S, E.A Davidson, and L.V. Verchot, Estimation of global biogeochemical controls and seasonality in soil methane consumption, *Chemosphere, 32*, 2219-2245, 1996b

Potter, C S, R H. Riley, and S.A. Klooster, Simulation modeling of nitrogen trace gas emissions along an age gradient of tropical forest soils, *Ecol. Model*, *97*, 179-196, 1997.

Prather, M J, R Derwent, D. Ehhalt, P. Fraser, E Sanhueza, and X. Zhou, Other trace gases and atmospheric chemistry, in *Climate Change 1994*, edited by J.T. Houghton et al., pp. 73-126, Cambridge Univ. Press, New York, 1995

Prather, M, R. Sausen, A Grossman, J Haywood, D Rind, and B H. Subbaraya, Potential climate change from aviation, in *Aviation and the Global Atmosphere*, edited by J E. Penner, et al, pp 185-215, Cambridge Univ Press, New York, 1999

Robertson, G P, and J M Tiedje, Nitrous-oxide sources in aerobic soils: Nitrification, denitrification and other biological processes, *Soil Biol. Biochem*, *19*, 187-193, 1987

Ryan, M G., R E McMurtie, G I. Ågren, E R Hunt Jr, J D Aber, A D Friend, E.B Rastetter, and W M Pulliam, Comparing models of ecosystem function for temperate conifer forests, II, Simulations of the effect of climate change, pp. 263-387, in *Global Change· Effects on Coniferous Forests and Grasslands, SCOPE vol. 56*, edited by A I Breymeyer et al, John Wiley, New York, 1996

Saxton, K E, W J Rawls, J S Romberger, and R I. Papendick, Estimating generalized soil-water characteristics from texture, *Soil Sci Soc Am J*, *50*, 1031-1036, 1986

Schimel, J P, M K Firestone, and K S Killham, Identification of heterotrophic nitrification in a Sierran forest soil, *Appl. and Environ Microbiol*, *48*, 802-806, 1984

Scholes, M C, R.E Martin, R.J. Scholes, D. Parsons, and E Winstead, NO and N_2O emissions from savanna soils following the first simulated rains of the season, *Nutr Cycling Agroecosyst*, *48*, 115-122, 1997

Schuster, M, and R. Conrad, Metabolism of nitric oxide and nitrous oxide during nitrification and denitrification in soil at different incubation conditions, *FEMS Microbiol. Ecol., 101*, 133-143, 1992.

Shao, Y, and A Henderson-Sellers, Validation of soil moisture simulation in land surface parameterization schemes with HAPEX data, *Global Planet. Change, 13*, 11-46, 1996.

Singh, B., B. Singh, and Y Singh, Potential and kinetics of nitrification in soils from semiarid regions of northwestern India, *Arid Soil Res Rehab., 7*, 39-50, 1993.

Skiba, U, K J Hargreaves, D. Fowler, and K.A Smith, Fluxes of nitric and nitrous oxide from agricultural soils in a cool temperate climate, *Atmos. Environ*, *26*, 2477-2488, 1992.

Slemr, F., and W Seiler, Field measurements of NO and N_2O emissions from fertilized and unfertilized soils, *J. Atmos. Chem., 2*, 1-24, 1984.

Smart, D.R, J.M Stark, and V. Diego, Resource limitation to nitric oxide emissions from a sagebrush-steppe ecosystem, *Biogeochemistry, 47*, 63-86, 1999.

Stark, J.M., Modeling the temperature response of nitrification, *Biogeochemistry*, 35, 433-445, 1996.

Veldkamp, E, and M Keller, Nitrogen oxide emissions from a banana plantation in the humid tropics, *J. Geophys. Res., 102*, 15,889-15,898, 1997

Veldkamp, E, M Keller, and M Nuñez, Effects of pasture management on N_2O and NO emissions from soils in the humid tropics of Costa Rica, *Global Biogeochem Cycles, 12*, 71-79, 1998.

Verchot, L.V, E.A. Davidson, J H. Cattanio, I L. Ackerman, H.E. Erickson, and M Keller, Land use change and biogeochemical controls of nitrogen oxide emissions from soils in eastern Amazonia, *Global Biogeochem. Cycles, 13*, 31-46, 1999.

Vitousek, P M, J D. Aber, R.H Howarth, G.E. Likens, P A. Matson, D W. Schindler, W.H. Schlesinger, and D.G Tilman, Human alteration of the global nitrogen cycle: Source and consequences, *Ecol. Appl*, *7*, 737-750, 1997.

Williams, E J, G L Hutchinson, and F Fesenfeld, NO_x and N_2O emissions from soil, *Global Biogeochem. Cycles, 6*, 351-388, 1992.

Yienger, J.J, and H Levy II, Empirical model of global soil biogenic NO_x emissions, *J Geophys. Res*, *100*, 11,447-11,464, 1995.

S. J. Del Grosso, M. D Hartmann, D. S Ojima, and W. J. Parton, Natural Resource Ecology Laboratory, Colorado State University, Fort Collins, CO 80523-1499. (delgro@nrel colostate.edu; melannie@nrel.colostate.edu; dennis@nrel colostate edu; billp@nrel. colostate.edu.)

E. A Holland and D. S. Schimel, Max Planck Institut fur Biogeochemie, Tatzendpromenade 1a, 07745 Jena, Germany. (eholland@bgc-jena mpg.de; dschimel@bgc-Jena mpg de.)

R. E. Martin, Cooperative Institute for Research in Environmental Sciences, University of Colorado, Boulder, CO 80309-0216. (Roberta.Martin@colorado edu)

A R Mosier, Agriculture Research Service, U S Department of Agriculture, P O. Box E, Fort Collins, CO 80522. (amosier@lamar. colostate.edu.)

(Received September 12, 2000; revised January 23, 2001; accepted January 26, 2001)